

Flower-like Surface Modification of Titania Materials by Lithium Hydroxide Solution

George Hasegawa,^{*,a} Kazuyoshi Kanamori,^a Yoshihiro Sugawara,^b Yuichi Ikuhara,^{b,c} and Kazuki Nakanishi^a

^a Department of Chemistry, Graduate School of Science, Kyoto University, Kitashirakawa, Sakyo-ku, Kyoto 606-8502, Japan

^b Japan Fine Ceramics Center, Mutsuno, Atsuta, Nagoya 456-8587, Japan

^c Institute of Engineering Innovation, School of Engineering, The University of Tokyo, Yayoi, Bunkyo-ku, Tokyo 113-8656, Japan

*Corresponding author: George Hasegawa

TEL/FAX: +81 757 537 673

E-mail: h_george@kuchem.kyoto-u.ac.jp

Abstract

Surface modification of titania materials to give flower-like structures has been achieved simply by the treatment in lithium hydroxide aqueous solution under mild conditions. The flower-like structured materials were characterized by X-ray diffraction, thermogravimetric analysis,

and Raman scattering. The analyses indicate that the flower-like materials are composed of layered hydrous lithium titanate. It is suggested that the unique intercalation behavior of lithium ions into titania allows dissolution and re-precipitation of titania to form the flower-like structure. The obtained flower-like structure can be retained up to 700 °C, while the crystal phase transforms into $\text{Li}_4\text{Ti}_5\text{O}_{12}$.

Keywords; surface modification, flower-like structure, titania, crystalline layered titanate, lithium intercalation

1. Introduction

Since the first report of water-splitting on titania (TiO_2) electrodes under ultraviolet (UV) light irradiation by Fujishima and Honda in 1972 [1], titania has attracted a lot of attention and substantial efforts have been made on the development of the titania-based materials and devices [2–16]. Owing to its unique characteristics [2,3], titania is currently one of the most promising materials in various fields, such as photovoltaic cells [6,7], photocatalysis [8], and separation science [9,10]. For effective application to these purposes, the nanostructure design of titania is of great importance [10–16]. For example, porous structure is required for separation media [10], catalysts [14,15], and electrodes [16] to provide accessible high surface area.

Recently, we have fabricated hierarchically porous titania monoliths by the sol–gel

technique accompanied by phase separation [17]. The control of the sol–gel reaction of titanium alkoxide can be achieved with the aid of chelating agent as well as appropriate electrolytes [18], while the phase separation is induced by the addition of poly(ethylene glycol). The immobilization of the co-continuous structure, which is formed in the course of spinodal decomposition, by the sol–gel transition provides well-defined interconnected macropores. The mesopores with relatively narrow size distributions are formed as the interstices of anatase crystallites, which are formed after the removal of the chelating agent, in the macropore skeletons. This porous titania monolith shows good separation performance for organophosphates [19].

For functionalization and/or structural modification of materials surfaces, post-modification techniques are useful. In most cases, the post-modification changes only the chemical nature, such as functional groups, of the materials surfaces [20-23]. Some post-modification can change not only the chemical nature but also the surface structure of the materials, which provides even superior functionality of materials [24,25]. In the case of titania materials, the post-modification in structure is remarkably difficult due to the excellent stability [26,27]. For example, it is known that the hydrothermal treatment in a strong alkaline solution ($>10 \text{ mol L}^{-1}$ NaOH or KOH) is necessary for the conversion of titania into layered titanates with nanotube and nanofiber structures [28–30]. This method, however, changes the whole titania material into nanotubes or nanofibers due to the harsh condition and is not available for the surface modification while keeping the porous structure.

In this research, the effects of the treatment in lithium hydroxide solution on the surface of the titania materials have been investigated. It was revealed for the first time that the treatment in lithium hydroxide aqueous solution under relatively mild conditions gives rise to the flower-like structure on the titania surface. This structural change is never observed when titania materials are treated in the other alkaline solution, such as ammonium hydroxide, sodium hydroxide, and potassium hydroxide [31,32], which indicates that the lithium ions have significant influence on this reaction. The flower-like structured material was characterized by X-ray diffraction, thermogravimetric analysis, and Raman scattering, and the formation mechanism of flower-like structure is discussed.

2. Experimental

2.1 Chemicals

Titanium (IV) *n*-propoxide ($\text{Ti}(\text{OPr})_4$) and polyethylene glycol (PEG, $M_v = 10\ 000$) were purchased from Sigma-Aldrich Co. (USA). Ethyl acetylacetonate (EtAcAc) and 1-propanol (PrOH) were purchased from Tokyo Chemical Industry Co., Ltd. (Japan). Ammonium nitrate (NH_4NO_3) and lithium hydroxide monohydrate ($\text{LiOH}\cdot\text{H}_2\text{O}$) were obtained from Kishida Chemical Co., Ltd. (Japan). All reagents were used as received. Distilled water was used in all experiments.

2.2 Preparation of titania monoliths

Porous titania monoliths were synthesized by the sol–gel method reported previously [17,19]. In a typical synthesis, 10 mL of $\text{Ti}(\text{OPr})_4$, 7.0 mL of PrOH and 5.0 mL of EtAcAc were mixed in a glass tube. After obtaining a homogeneous yellow solution, 0.875 g of PEG was added followed by stirring at 60 °C and PEG was completely dissolved. Then, the solution was cooled to 40 °C and 2.0 mL of 1 mol L^{-1} NH_4NO_3 aq. was added slowly with vigorous stirring. After mixing for 3 min, the obtained homogeneous solution was kept at 40 °C for 24 h. The obtained gels were sequentially immersed in the following solutions in a loosely closed container at 60 °C: ethanol (EtOH), $\text{EtOH}/\text{H}_2\text{O} = 1/1$, and H_2O . Each immersion time was 24 h. The chelating agent, EtAcAc , was removed by hydrolysis and decarbonation through this process, which also promotes the formation of anatase crystallites [17]. The obtained wet titania gels were dried at 60 °C. The calcined titania monoliths were obtained by the calcination of the dried titania monoliths at different temperatures for 2 h.

2.3 Preparation of titania particles

For preparing titania particles, 5.0 mL of $\text{Ti}(\text{OPr})_4$ and 10 mL of PrOH were mixed in a glass tube. Then, 1.0 mL of H_2O was added slowly with vigorous stirring at 0 °C. After the solution became opaque, the temperature was raised to room temperature and the solution was stirred for 1 h. The resultant precipitants were washed with H_2O followed by drying at 60 °C.

2.4 Surface modification

For the treatment with LiOH aq., the wet titania gels (after washing with H₂O) were immersed in various concentrations of LiOH aq. at various temperatures in polypropylene containers. When the treatment temperature was more than 80 °C, the reaction was performed in an autoclave to inhibit the vaporization and the change of the concentration of LiOH aq. The resultant samples were washed with H₂O at 60 °C for 3 h for five times in order to remove the excess Li ions. After evaporative drying at 60 °C, the dried surface-modified titania monoliths and particles were obtained. Some samples were subsequently calcined at various temperatures for 2 h. The dried and calcined titania monoliths as well as the titania particles were also subjected to the same process.

2.5 Characterization

Observation of the microstructures of the fractured surfaces of the samples was conducted under scanning electron microscopy (SEM) (JSM-6060S, JEOL, Japan), field emission scanning electron microscopy (FE-SEM) (JSM-6700F, JEOL, Japan) and transmission electron microscopy (TEM) (JEM-2010DM, JEOL, Japan). The crystal structure was confirmed by powder X-ray diffraction (XRD) (RINT Ultima III, Rigaku Corp., Japan) using Cu K α ($\lambda = 0.154$ nm) as an incident beam. Nitrogen adsorption–desorption (BELSORP-mini II, Bel Japan Inc., Japan) was employed to characterize the meso- and micropores of the samples. Before nitrogen adsorption-desorption measurements, the samples were calcined at 200 °C for 2 h followed by being degassed under vacuum at 150 °C for more than 6 h. Thermogravimetric (TG) analysis was

performed by Thermo plus TG 8120 (Rigaku Corp., Japan) at a heating rate of $5\text{ }^{\circ}\text{C min}^{-1}$. The titania particles were dried under vacuum to remove the adsorbed water before the measurement. In order to avoid the adsorption of water, the TG analysis was performed under argon atmosphere by supplying argon at a rate of 100 mL min^{-1} . Raman spectrum of the sample was measured using a Jobin-Yvon T-6400 spectrometer (HORIBA, Ltd., Japan). The incident light used for the experiments was the 514.5 nm Ar line of the laser source (GLG3260, NEC Corp., Japan).

3. Results and Discussion

3.1 Effect of the concentration of LiOH aq. and the treatment temperature

Figure 1 a and b show the change in structure of the titania monoliths by the treatment in 0.8 mol L^{-1} LiOH aq. at $80\text{ }^{\circ}\text{C}$ for 24 h. The flower-like structure was formed with the platy crystallites on the titania surface with maintaining the macroporous structure. In addition, the crack-free monolithicity can also be retained as shown in the inset of Figure 1 b. The SEM images of the samples with the different treatment times are shown in Figure S1. It is found that the platy crystallites become visible after the treatment for 5 h. Comparing the samples treated for 6 h and 24 h, number density of the platy crystallites is similar and the crystal size becomes larger with increasing the treatment time. When fixing the treatment temperature at $80\text{ }^{\circ}\text{C}$, the flower-like structure was formed with the LiOH-concentrations of $0.4\text{--}0.8\text{ mol L}^{-1}$ as shown in Figure S2. On the other hand, when fixing the concentration of LiOH aq. in 0.8 mol L^{-1} , the flower-like structure was formed by the treatment at $60\text{--}80\text{ }^{\circ}\text{C}$ as shown in Figure S3. The results of the surface

modification treated in various concentrations of LiOH aq. and at various temperatures are summarized in Figure 1 c, which indicates that the surface modification of titania materials is possible under defined conditions. As decreasing the concentration of LiOH aq., the flower-like structure was formed when the titania monoliths were treated at higher temperatures. The XRD patterns of the samples treated under various conditions are shown in Figure S4. When the treatment condition is weaker than 0.4 mol L^{-1} LiOH aq. at $60 \text{ }^\circ\text{C}$, no change in diffraction patterns was observed. On the other hand, when the treatment condition is stronger than 0.8 mol L^{-1} LiOH aq. at $80 \text{ }^\circ\text{C}$, the XRD patterns exhibit an obvious change; most of anatase changes to LiTiO_2 as reported previously [33]. It is also found that all XRD patterns of the samples with the flower-like structure include the same peaks of layered hydrous lithium titanate (LHLT) except for those of anatase, which will be discussed later.

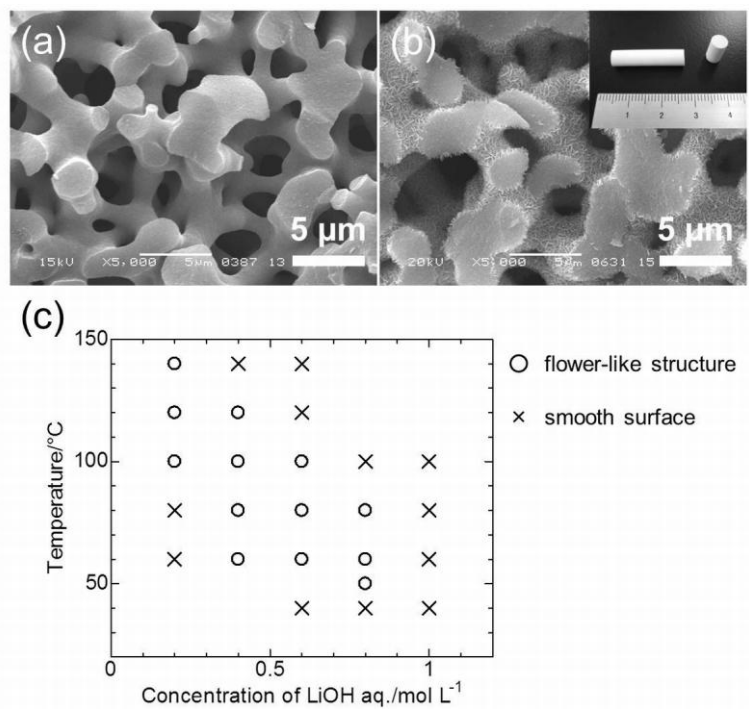


Figure 1 SEM images of the dried titania monolith (a) before and (b) after the treatment in 0.8 mol L⁻¹ LiOH aq. at 80 °C for 24 h. The inset of (b) is the appearance of the surface-modified titania monolith. (c) Results of the treatment under various conditions for 24 h. The platy crystallites were observed under SEM with the conditions designated as “flower-like structure” and no change was observed with the conditions as “smooth surface”.

Figure 2 a and b show the SEM images of the surface-modified samples which were subjected to the calcination at 700 °C and 800 °C, respectively. It is found that the obtained flower-like structure was retained up to 700 °C. The XRD patterns of the calcined surface-modified titania monoliths are shown in Figure 2 c. The peaks which are attributed to

LiTiO₂ are observed in the sample calcined at 200 °C, while the peaks related to Li₄Ti₅O₁₂ are observed in the samples calcined above 400 °C. It is notable that the peaks of anatase presumably from the skeletons of the macropores still remain even after the calcination at 700 °C. The magnified image of the cross section of the skeleton also indicates that the platy materials appear only on the surface of the skeletons and that no change is observed in the inner part of the titania skeleton as shown in Figure 3 a. Figure 3 b and Table 1 show the micro- and mesopore characteristics of the titania monolith with and without the surface modification. The micro- and mesopore volume and the specific surface area slightly decreased by the surface modification due to the densification during the treatment and to the introduction of Li ions, which increases density of the titania monoliths. Most of the micro- and mesopores are deduced to derive from the original skeletons, not from the flower-like structure, which indicates that the pores of the anatase skeletons are still accessible even after the surface modification. For practical applications of this technique, it should be emphasized that the anatase phase, which shows excellent photocatalytic and bioseparation properties [2,3,6–10,19], can be retained as the major constituent in the material. For example, the resultant surface-modified macroporous titania monoliths may be utilized as the separation media [10,19] with the additional function of ion-exchange ability. Besides, the surface modification on titania films (see Figure S5) for optical devices such as photocatalyst and photovoltaic cells, we can provide functionality such as anti-reflection [25] and water repellency [34], which can be derived from the flower-like structured coating, without losing the photoactivity of anatase.

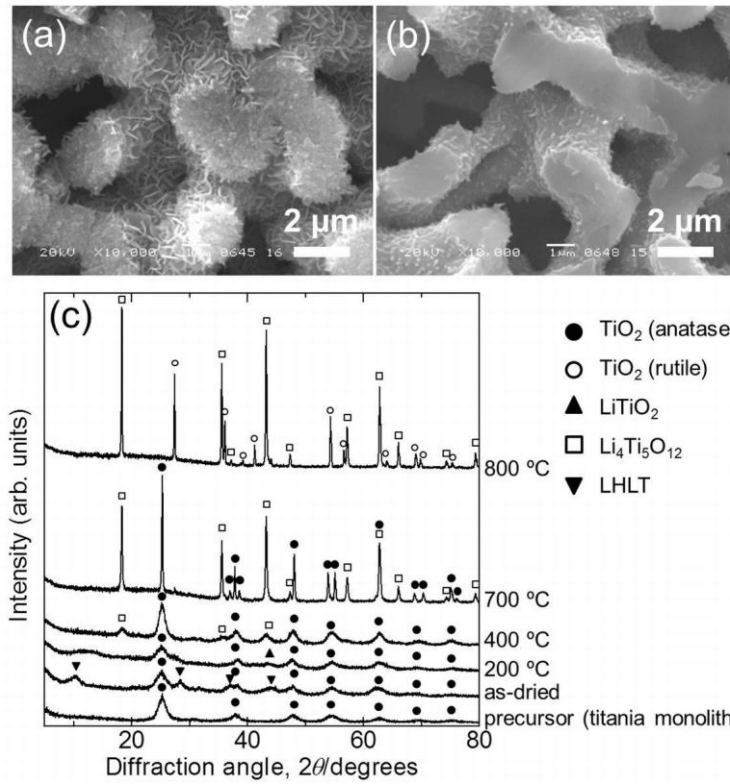


Figure 2 SEM images of the titania monoliths calcined at (a) 700 °C and (b) 800 °C. (c) XRD patterns of the surface-modified titania monoliths calcined at different temperatures.

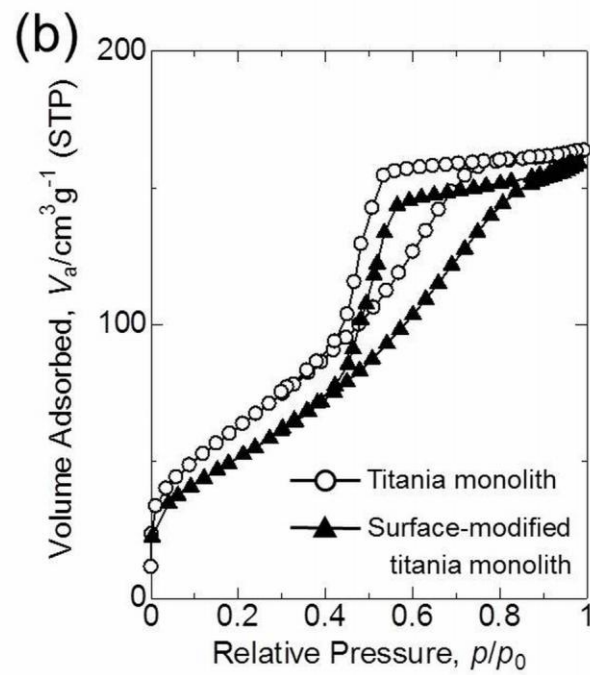
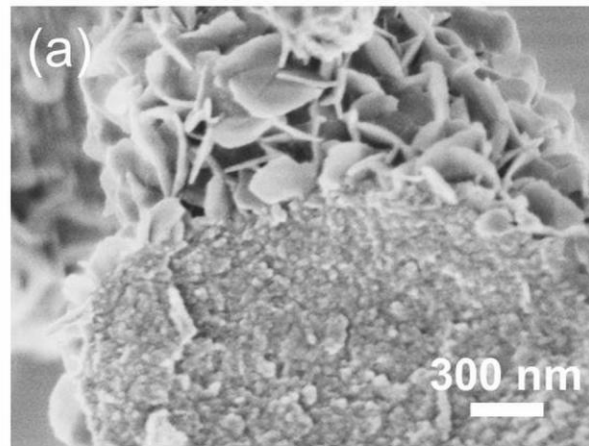


Figure 3 (a) FE-SEM image of the cross section of the skeleton in the surface-modified titania monolith. (b) Nitrogen adsorption-desorption isotherms of the titania monoliths with and without the surface modification.

Table 1 Pore characteristics of the titania monoliths with and without the surface modification.

	$V_p^a/\text{cm}^3 \text{ g}^{-1}$	$S_{\text{BET}}^b/\text{m}^2 \text{ g}^{-1}$	D_p^a/nm
Titania monolith	0.253	220	5.5
Surface-modified titania monolith	0.246	190	5.5

^aTotal pore volumes V_p and mean pore diameter D_p obtained by the BJH method using adsorption branch. ^b Specific surface areas calculated by BET method.

3.2 Material characterization

Characterizations of the platy materials were performed utilizing the particle samples prepared from the titania particles ($\sim 1 \mu\text{m}$). Figure 4 shows the FE-SEM and TEM images of the particle samples after the treatment in 0.8 mol L^{-1} LiOH aq. at $80 \text{ }^\circ\text{C}$ for 24 h. Starting from titania particles, the aggregates of platy crystallites were obtained. The thickness of each plate is about 30 nm. Unfortunately, it was found that TEM and electron diffraction are not available for the determination of crystal structure of the dried sample because the crystal phase changed during the observation due to the low thermal stability. The XRD patterns of the dried samples and samples calcined at different temperatures are shown in Figure 5 a. Comparing the XRD patterns of the as-dried sample prepared from titania monolith and titania particles, the platy materials on the surface of the titania monoliths are the same with those on the particles. All peaks except for the small peak of anatase (101) are attributed to LHLT [35,36]. The diffraction peak at $2\theta \sim 10.5^\circ$ derives from the interlayer spacing of titanate [29,37]. The TG analysis result (Figure 5 b) also indicates that the flower-like crystals include some crystal water, which causes the thermal

instability of LHLT. The Raman spectrum of the as-dried powder shows four characteristic bands centered at 278, 435, 689, and 858 cm^{-1} as shown in Figure 5 c. The bands in the 250-400 cm^{-1} region and 400-700 cm^{-1} region correspond to the Li-O stretches of LiO_6 octahedra and LiO_4 tetrahedra, respectively [38,39]. The bands in the 550-700 cm^{-1} region are assigned to Ti-O stretches in TiO_6 octahedra [38,39]. The Raman scattering result indicates that the lithium ions occupy both octahedral and tetrahedral positions. The XRD patterns also show that the calcination at 200 $^{\circ}\text{C}$ changes the crystallites into LiTiO_2 and the unidentified phase because of the loss of crystal water as shown in the TG result. The main crystal phase transforms into the spinel $\text{Li}_4\text{Ti}_5\text{O}_{12}$ [36], which is known as the anode material for Li-ion battery [33,36], after the calcination above 300 $^{\circ}\text{C}$.

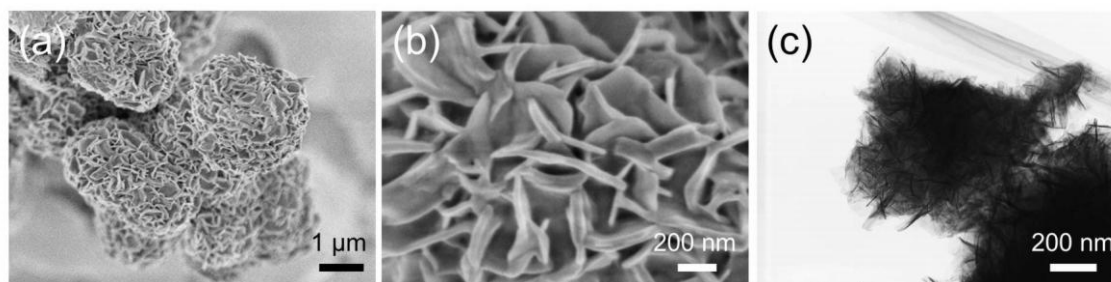


Figure 4 FE-SEM images (a,b) and TEM bright field image (c) of the dried sample prepared from the titania particles.

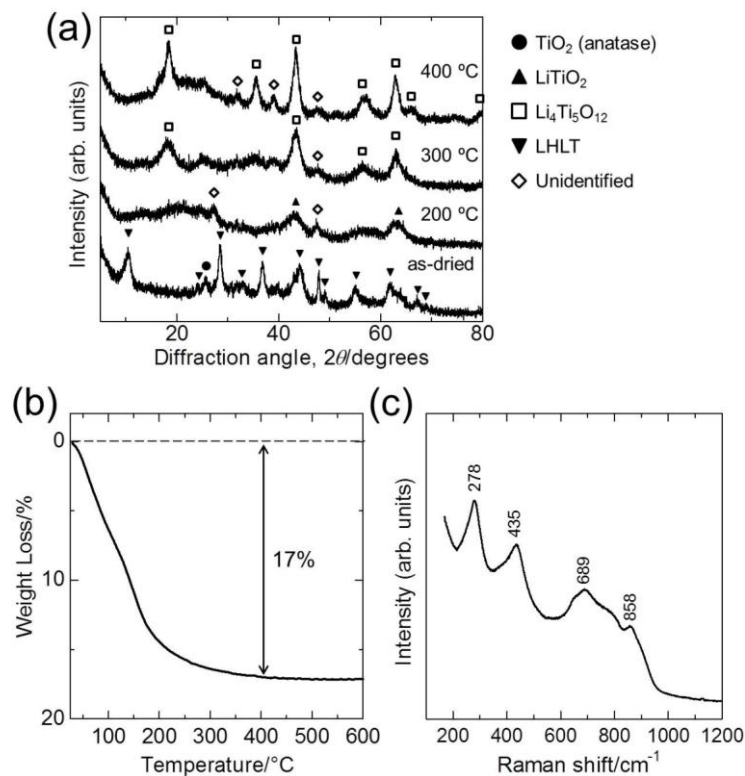


Figure 5 (a) XRD patterns of the dried and calcined particle samples. (b) TG analysis result of the dried sample prepared from the titania particles. (c) Raman spectrum of the dried sample prepared from the titania particles.

3.3 Proposed mechanism

The suggested formation mechanism of the crystallites is based on dissolution and re-precipitation. Many theoretical and electrochemical studies inform that Li ions can be easily intercalated due to the small ion size [40-42]. Therefore, Li ions would penetrate into the anatase crystallites from the surface. Then, the intercalated Li ions expand the Ti-O lattice

to some extent [40,41], which enhances the solubility of titania. The dissolved species re-precipitate with the surrounding Li ions as well as H₂O resulting in the formation of layered hydrous lithium titanate crystallites on the surface of the titania material. When the treatment condition is weak, the dissolution does not occur, resulting in no change on the titania surface. On the other hand, when the treatment condition is strong, the anatase phase is directly transformed into LiTiO₂ without forming platy crystallites.

3.4 Effect of titania crystallinity on surface modification

The surface modification process was also tried using the dried and the calcined titania monoliths instead of the wet gels as shown in Figure 6. The precursor titania monolith calcined at 700 °C was composed of rutile and the others were composed of anatase as shown in Figure S6. It is found that the surface modification of flower-like structure was achieved even with the titania monolith calcined at 500 °C. On the other hand, there are only a few platy materials observed when starting from the sample calcined at 600 °C and there is no platy ones in the case of the rutile monolith. Comparing the titania monoliths calcined at 500 °C and 600 °C, the difference is deduced to derive from the anatase crystallite size and the crystallinity of anatase in the precursors. The crystallite size of the titania monoliths calcined at 500 °C and 600 °C are calculated as *ca.* 10 nm and *ca.* 30 nm by Scherrer's equation. The crystallinity of the titania monoliths calcined at higher temperature is higher. The larger crystallites with

higher crystallinity lead to the slower intercalation of Li ions [42] and less solubility, which supresses the formation of platy crystallites. In the case of the rutile monolith, the intercalation of Li ions into rutile takes place slower than that into anatase [40]. Hence, the surface modification is not effective for the rutile material. It is also observed that the size of the platy objects changed depending on the precursors. Starting from the dried and calcined samples, the sizes of each plate are obviously larger compared to the case of the sample prepared using the wet titania gel. This fact can be explained by the roughness of the surface of the precursor. The surface of the dried monolith is smoother than that of the wet gel due to the densification during drying caused by the surface tension. The smoother surface leads to the less nucleation cites, which indicates that less crystal nuclei are formed in the initial period of re-precipitation. Each crystallite therefore grows up better resulting in the larger platy crystallites in the case of the dried and calcined titania monoliths.

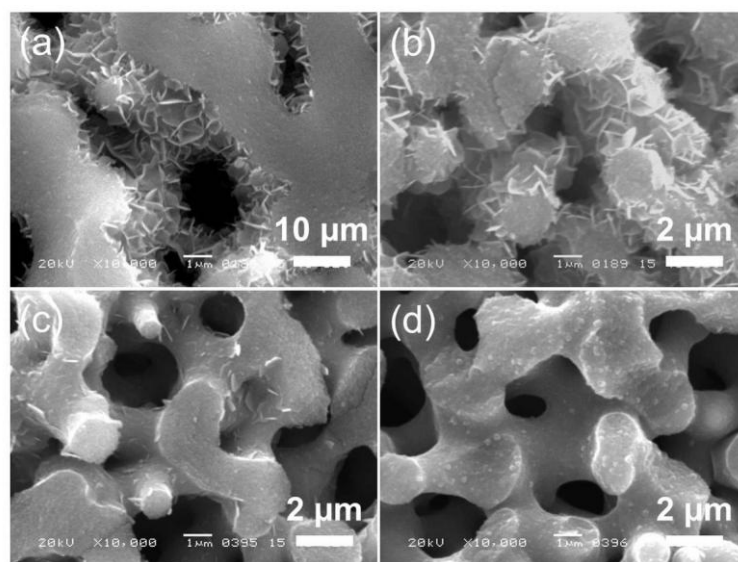


Figure 6 SEM images of the surface-modified titania monoliths prepared from (a) the dried titania and the titania monoliths calcined at (b) 500 °C, (c) 600 °C, and (d) 700 °C.

4. Conclusions

We have found a unique reaction can occur on the surface of titania materials in lithium hydroxide aqueous solution, which can be applied to the surface modification of titania materials. Under weak treatment conditions, no change in structure or crystal phase occurs on titania materials. On the other hand, when the treatment conditions are relatively strong, transformation into LiTiO_2 with no structural change is observed [32,33]. These flower-like structures form on the surface of titania materials under intermediate conditions. This structure retains after calcination at up to 700 °C whereas the crystal phase transforms into $\text{Li}_4\text{Ti}_5\text{O}_{12}$. The as-dried platy materials which form the flower-like structures have been identified as layered hydrous lithium titanate [35,36]. The formation of the flower-like structures is based on dissolution and re-precipitation. It is deduced that the high intercalation properties of small Li ions cause the dissolution of titania under mild conditions. When the titania materials are composed of large anatase or rutile with high crystallinity, the structural change was not observed due to the poor dissolution of titania.

Acknowledgement

The present work was supported by the Grant-in-Aid for Scientific Research (No. 22·75 for G.H.

and No. 20750177 for K.K.) from the Ministry of Education, Culture, Sports, Science and Technology (MEXT), Japan. Also acknowledged is the Global COE Program "International Center for Integrated Research and Advanced Education in Materials Science" (No. B-09) of the MEXT, Japan, administrated by the Japan Society for the Promotion of Science (JSPS).

References

- [1] A. Fujishima, K. Honda, *Nature* 238 (1972) 37.
- [2] H. Tang, K. Prasad, R. Sanjinés, P.E. Schmid, F. Lévy *J. Appl. Phys.* 75 (1994) 2042.
- [3] A. L. Linsebigler, G. Lu, J. T. Yates, Jr., *Chem. Rev.* 95 (1995) 735.
- [4] S.-D. Mo, W.Y. Ching, *Phys. Rev. B* 51 (1995) 13023.
- [5] R. Marchand, L. Brohan, M. Tournoux, *Mat. Res. Bull.* 15 (1980) 1129.
- [6] M. Grätzel, *Nature* 414 (2001) 338.
- [7] N.-G. Park, J. van de Lagemaat, A.J. Grank, *J. Phys. Chem. B* 104 (2000) 8989.
- [8] M.R. Hoffmann, S.T. Martin, W. Choi, W. Bahnemann, *Chem. Rev.* 95 (1995) 69.
- [9] M.W.H. Pinkse, P.M. Uitto, M.J. Hilhorst, B. Ooms, A.J.R. Heck, *Anal. Chem.* 76 (2004) 3935.
- [10] J. Konishi, K. Fujita, K. Nakanishi, K. Hirao, K. Morisato, S. Miyazaki, M. Ohira, *J. Chromatogr. A* 1216 (2009) 7375.
- [11] Y. Zhou, M. Antonietti, *J. Am. Chem. Soc.* 125 (2003) 14960.
- [12] Z. Zhong, Y. Yin, B. Gates, Y. Xia, *Adv. Mater.* 12 (2000) 206.
- [13] D. Chen, L. Cao, F. Huang, P. Imperia, Y.-B. Cheng, R.A. Caruso, *J. Am. Chem. Soc.* 132 2010

4438.

[14] J.D. Bass, D. Grosso, C. Boissiere, C. Sanchez, *J. Am. Chem. Soc.* 130 (2008) 7882.

[15] H. Li, Z. Bian, J. Zhu, D. Zhang, G. Li, Y. Huo, H. Li, Y. Lu, *J. Am. Chem. Soc.* 129 (2007) 8406.

[16] Y.-G. Guo, Y.-S. Hu, W. Sigle, J. Maier, *Adv. Mater.* 19 (2007) 2087.

[17] G. Hasegawa, K. Kanamori, K. Nakanishi, T. Hanada, *J. Am. Ceram. Soc.* 93 (2010) 3110.

[18] G. Hasegawa, K. Kanamori, K. Nakanishi, T. Hanada, *J. Sol-Gel Sci. Technol.* 53 (2010) 59.

[19] G. Hasegawa, K. Morisato, K. Kanamori, K. Nakanishi, *J. Sep. Sci.* 34 (2011) 3004.

[20] J.R. Conrad, J.L. Radtke, R.A. Dodd, F.J. Worzala, N.C. Tran, *J. Appl. Phys.* 62 (1987) 4591.

[21] J.L. Figueiredo, M.F.R. Pereira, M.M.A. Freitas, J.J.M. Órfão, *Carbon* 37 (1999) 1379.

[22] H. Minakuchi, K. Nakanishi, N. Soga, N. Ishizuka, N. Tanaka, *Anal. Chem.* 68 (1996) 3498.

[23] X.S. Zhao, G.Q. Lu, *J. Phys. Chem. B* 102 (1998) 1556.

[24] K. Kato, E. Uchida, E.T. Kang, Y. Uyama, Y. Ikeda, *Prog. Polym. Sci.* 28 (2003) 209.

[25] N. Yamaguchi, K. Tadanaga, A. Matsuda, T. Minami, M. Tatsumisago, *J. Sol-Gel Sci. Technol.* 33 (2005) 117.

[26] H. Zhang, J.F. Banfield, *J. Mater. Chem.* 8 (1998) 2073.

[27] J. Nawrocki, C. Dunlap, A. McCormick, P.W. Carr, *J. Chromatogr. A* 1028 (2004) 1.

[28] T. Kasuga, M. Hiramatsu, A. Hoson, T. Sekino, K. Niihara, *Langmuir* 14 (1998) 3160.

[29] A.R. Armstrong, G. Armstrong, J. Canales, P.G. Bruce, *Angew. Chem. Int. Ed.* 43 (2004) 2286.

[30] Y. Lan, X. Gao, H. Zhu, Z. Zheng, T. Yan, F. Wu, S.P. Ringer, D. Song, *Adv. Funct. Mater.* 15

(2005) 1310.

[31] M. Tomiha, N. Masaki, S. Uchida, T. Sato, *J. Mater. Sci.* 37 (2002) 2341.

[32] L.M. Sikhwivhilu, S.S. Ray, N.J. Coville, *Appl. Phys. A* 94 (2009) 963.

[33] C. Jiang, E. Hosono, M. Ichihara, I. Honma, H. Zhou, *J. Electrochem. Soc.* 155 (2008) A553.

[34] T. Onda, S. Shibuichi, N. Satoh, K. Tsujii, *Langmuir* 12 (1996) 2125.

[35] M. Sugita, M. Tsuji, M. Abe, *Bull. Chem. Soc. Jpn.* 63 (1990) 1978.

[36] Y. Tang, L. Yang, S. Fang, Z. Qiu, *Electrochim. Acta* 54 (2009) 6244.

[37] R. Yoshida, Y. Suzuki, S. Yoshikawa, *J. Solid State Chem.* 178 (2005) 2179.

[38] T. Nakazawa, V. Grismanovs, D. Yamaki, Y. Katano, T. Aruga, *Nucl. Instrum. Methods Phys. Res. B* 206 (2003) 166.

[39] L. Aldon, P. Kubiak, M. Womes, J.C. Jumas, J. Olivier-Fourcade, J.L. Tirado, J.I. Corredor, C.P. Vicente, *Chem. Mater.* 16 (2004) 5721.

[40] A. Stashans, S. Lunell, R. Bergström, A. Hagfeldt, S.-E. Lindquist, *Phys. Rev. B* 53 (1996) 159.

[41] R. van de Krol, A. Goossens, J. Schoonman, *J. Phys. Chem. B* 103 (1999) 7151.

[42] M. Wagemaker, W.J.H. Borghols, F.M. Mulder, *J. Am. Chem. Soc.* 129 (2007) 4323.

Supporting Information

Flower-like Surface Modification of Titania Materials

by Lithium Hydroxide Solution

By George Hasegawa,* Kazuyoshi Kanamori, Yoshihiro Sugawara, Yuichi Ikuhara, and Kazuki

Nakanishi

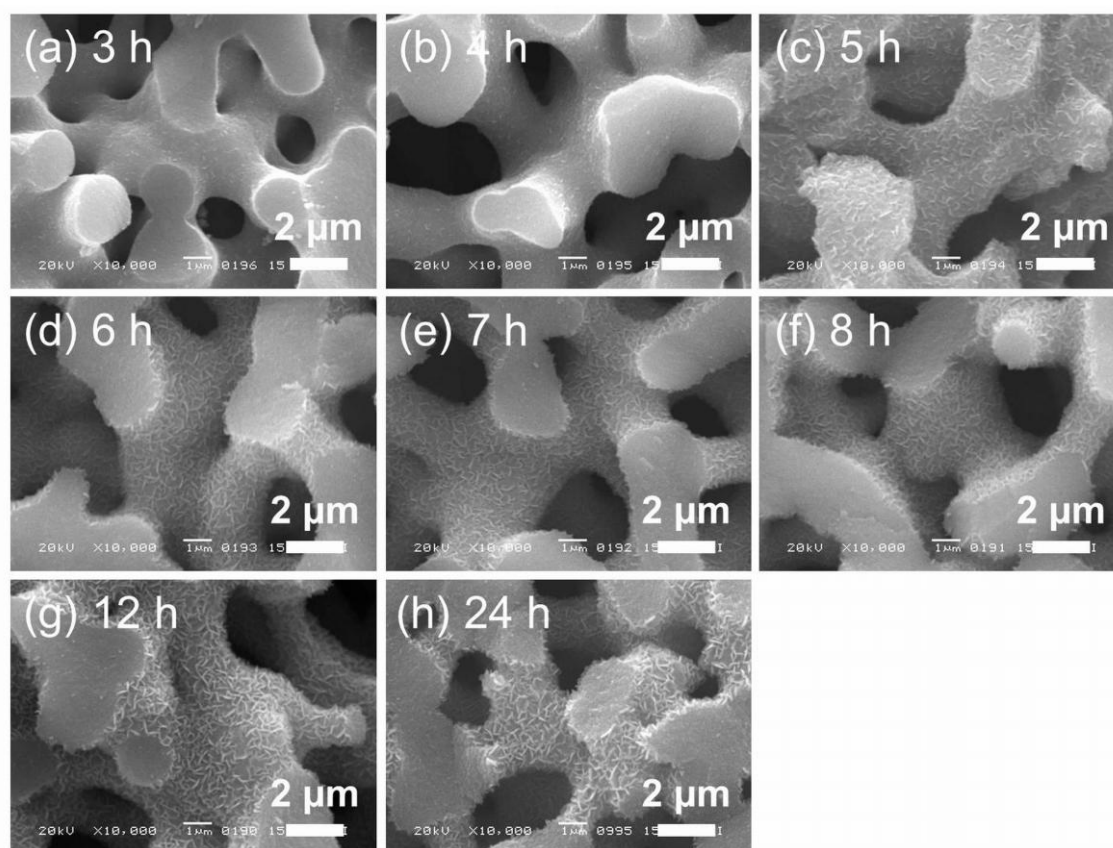


Figure S1 SEM images of the titania monoliths after the treatment in 0.8 mol L⁻¹ LiOH aq. at 80 °C for different durations.

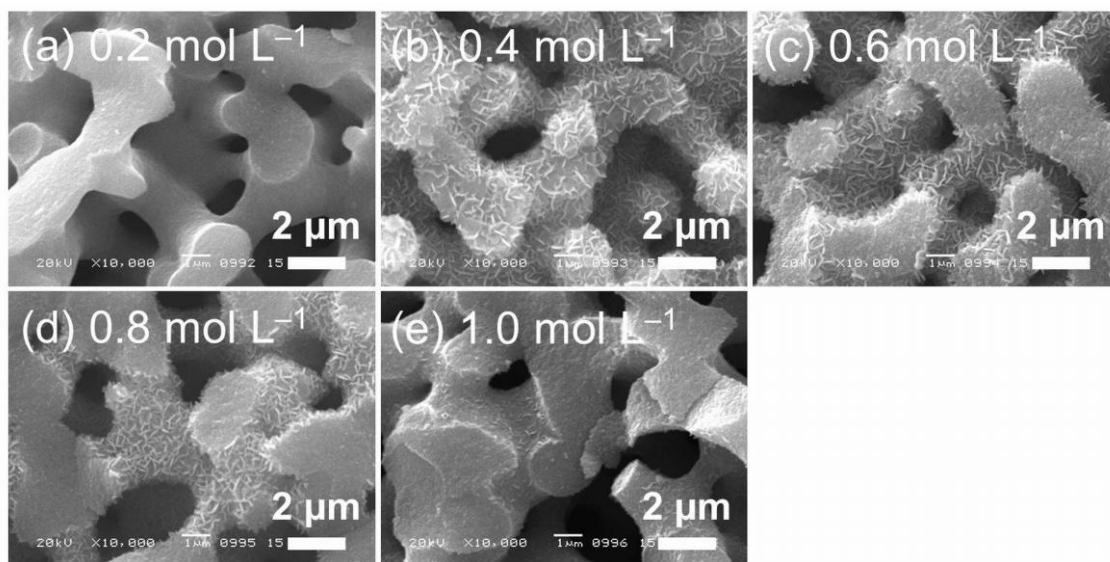


Figure S2 SEM images of the titania monoliths after the treatment in different concentrations of LiOH aq. at 80 °C for 24 h.

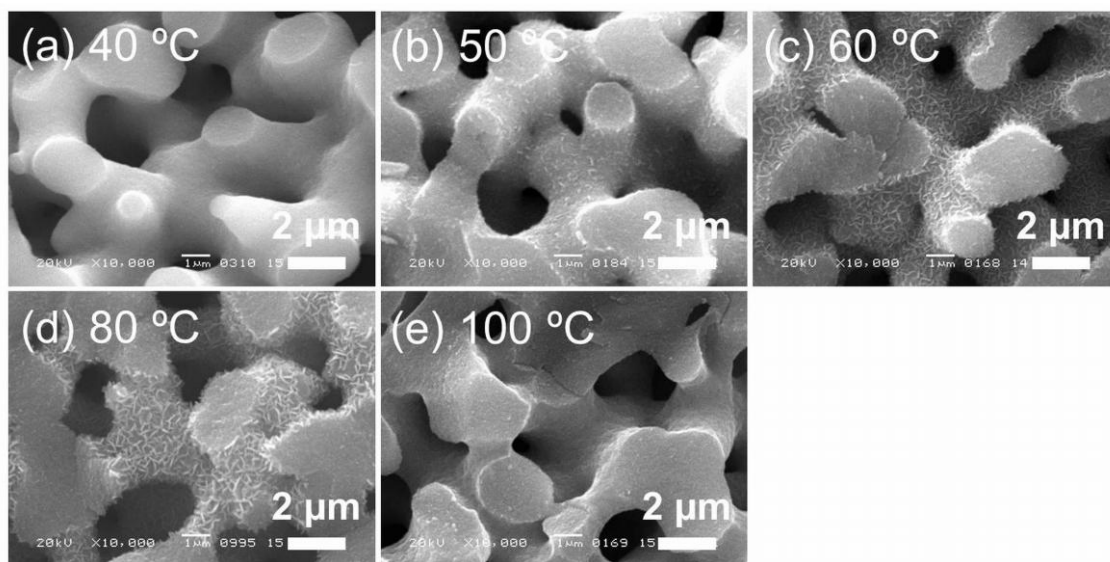


Figure S3 SEM images of the titania monoliths after the treatment in 0.8 mol L⁻¹ LiOH aq. at different temperatures for 24 h.

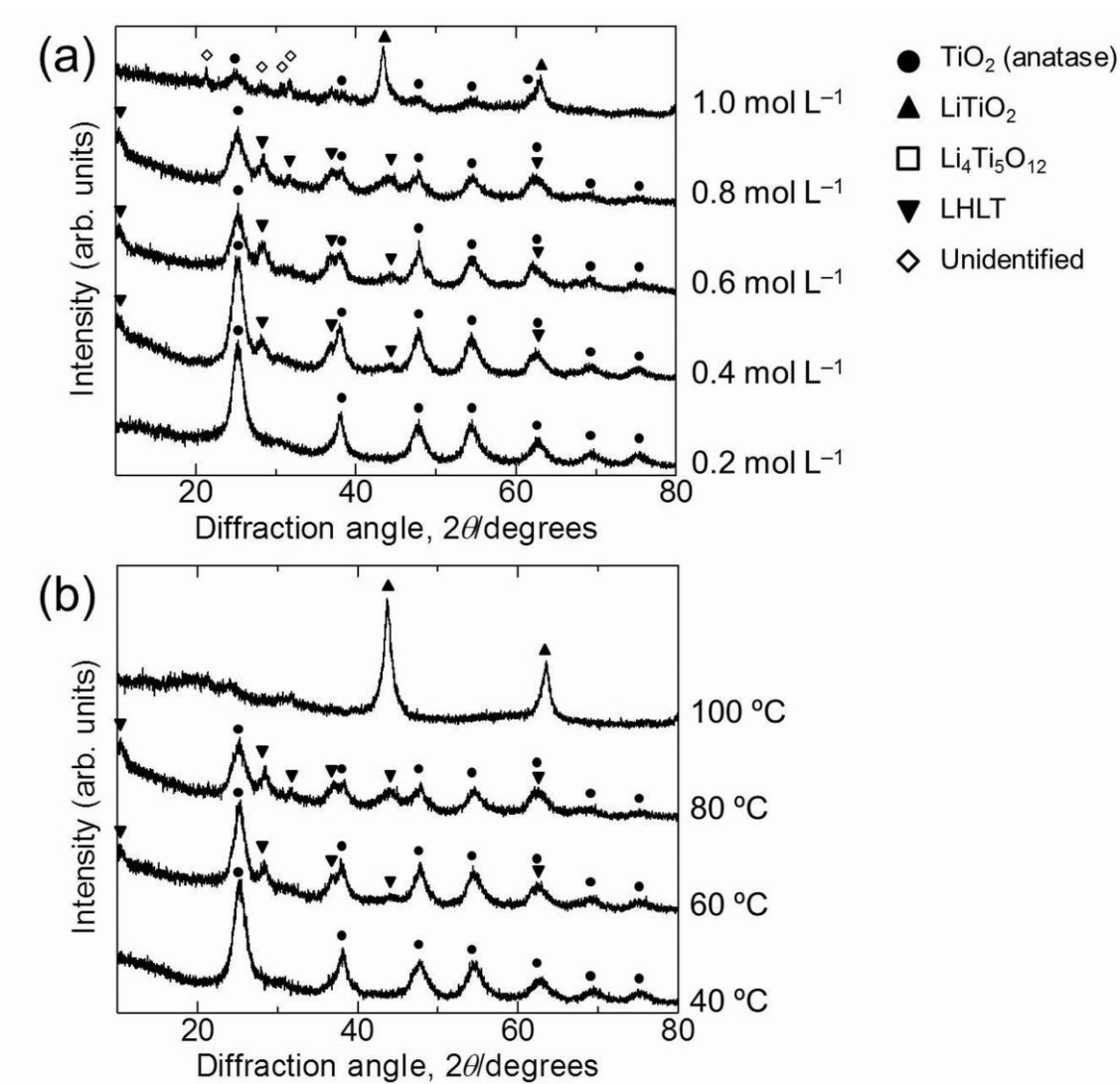


Figure S4 XRD patterns of the titania monoliths treated in various conditions; (a) treated in various concentrations of LiOH aq. at 80 °C for 24 h and (b) treated in 0.8 mol L⁻¹ LiOH aq. at various temperatures for 24 h.

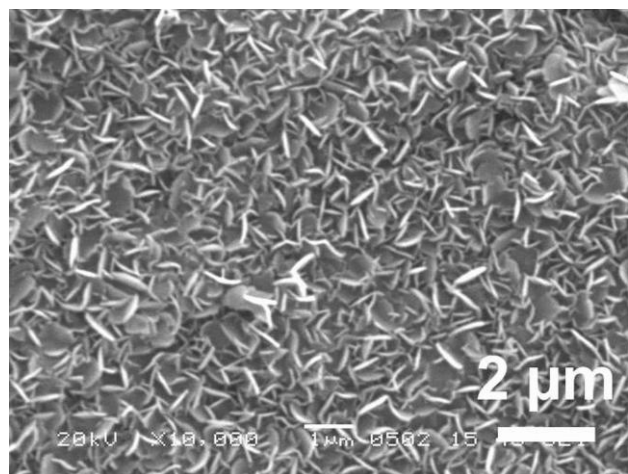


Figure S5 SEM image of the flower-like structure on the flat titania surface.

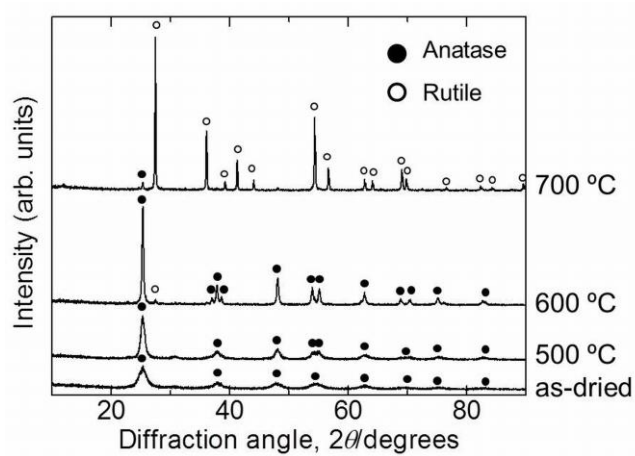


Figure S6 XRD patterns of the precursor titania monoliths which has been dried and calcined.